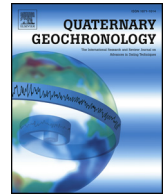




ELSEVIER

Contents lists available at ScienceDirect

# Quaternary Geochronology

journal homepage: [www.elsevier.com/locate/quageo](http://www.elsevier.com/locate/quageo)

Research paper

## OSL surface exposure dating of a lithic quarry in Tibet: Laboratory validation and application

L.A. Gliganic<sup>a,\*</sup>, M.C. Meyer<sup>a</sup>, R. Sohbati<sup>b</sup>, M. Jain<sup>b</sup>, S. Barrett<sup>a</sup><sup>a</sup> Institute for Geology, University of Innsbruck, Innrain 52, 6020 Innsbruck, Austria<sup>b</sup> Center for Nuclear Technologies, Technical University of Denmark, DTU Risø Campus, Roskilde, Denmark

### ABSTRACT

Recent work has shown that the optically stimulated luminescence (OSL) signal can be used to determine the duration of daylight exposure for rock surfaces, complementing the surface exposure dating technique using cosmogenic nuclides. In this study we investigate the feasibility of using the newly developed OSL Surface exposure dating technique (OSL-Surf) to date flake scars at lithic quarry sites. We performed the first quantitative validation of the model describing the OSL-Surf dating technique using a controlled laboratory experiment. Our results show that longer laboratory bleaching durations yield deeper OSL-depth profiles, validating the use of OSL-Surf approach for relative dating of rock surfaces with different exposure ages. The OSL-surf model fitted to the OSL-depth profiles (excluding one outlier) yields accurate estimates of known exposure duration, thus confirming the method's usefulness as an absolute dating tool. Consequently, we used the OSL-Surf technique to determine an exposure duration of  $117 \pm 37$  a for a previously unknown-age flake scar that is related to human exploitation of a lithic quarry site in Tibet. The problem of finding a known-age rock surface for parameter calibration was solved by revisiting the sampling site and collecting the scar remaining after earlier sample collection, which has a precisely known exposure age (1.667 a in this study) and identical lithology and irradiation aspect as the flake scar. The calibration sample yielded a measurable OSL-depth profile that could be used to calibrate the model to estimate the exposure duration of a flake scar associated with human exploitation of the area. Finally, we observe that the  $\mu$  parameter of the OSL-Surf model varies considerably between the laboratory-bleached and two naturally daylight-bleached datasets, despite having identical lithologies. We thus infer that, in addition to lithological controls, the  $\mu$  parameter is primarily sensitive to the daylight irradiation geometry and only weakly dependent on spectrum of the incident light; this interpretation implies a narrow effective bleaching wavelength band in quartzite. From the practical viewpoint, our results suggest that geometrical factors deserve a careful consideration both while designing the laboratory bleaching experiments as a surrogate of natural bleaching, as well as while choosing the field calibration samples.

### 1. Introduction

The optically stimulated luminescence (OSL) signal from mineral grains is normally used to date the amount of time for which sediment grains were buried. However, recent work has shown that luminescence signals can also be used to determine the duration of daylight exposure for rock surfaces (Laskaris and Liritzis, 2011; Sohbati et al., 2011, 2012a). This approach provides similar but complementary information to surface exposure dating using cosmogenic nuclides (CN); the signal in CN surface exposure dating develops over a few hundreds of centimetres of material and is applicable over relatively long time scales ( $\sim 10^4$ – $10^6$  a), whereas the OSL surface exposure dating signal develops in a few centimetres of material and is detectable on rather short time

scales ( $\sim 10^{-4}$ – $10^4$  a).

The OSL surface exposure dating (henceforth, OSL-Surf) technique is based on the depth-dependence of the resetting (bleaching) of the latent luminescence signal when exposed to daylight. Sohbati et al. (2011, 2012a, 2012b) proposed that the dependence of the OSL signal on depth and exposure-time could be described by a double exponential function:

$$L = L_0 e^{-\frac{x}{\sigma\phi_0} t} e^{-\mu x} \quad (1)$$

where  $L$  is the luminescence signal measured at depth  $x$  (mm) after exposure time  $t$  (s) and  $L_0$  is the luminescence signal in field saturation.  $\frac{x}{\sigma\phi_0}$  ( $s^{-1}$ ) is the effective detrapping-rate constant describing an integral of the product of the wavelength-dependent photo-ionisation

\* Corresponding author.

E-mail address: [luke.gliganic@uibk.ac.at](mailto:luke.gliganic@uibk.ac.at) (L.A. Gliganic).<https://doi.org/10.1016/j.quageo.2018.04.012>

Received 5 December 2017; Received in revised form 27 February 2018; Accepted 27 April 2018

1871-1014/ © 2018 The Authors. Published by Elsevier B.V. This is an open access article under the CC BY license (<http://creativecommons.org/licenses/by/4.0/>).

cross section ( $\sigma$ ;  $\text{cm}^2$ ) and photon flux at the rock surface ( $\phi_0$ ;  $\text{cm}^{-2}\text{s}^{-1}$ ).  $\mu$  ( $\text{mm}^{-1}$ ) is the attenuation coefficient characterising light penetration into the rock. This model is based on first-order kinetics for luminescence decay and an exponential attenuation of light intensity with depth, and it predicts that the longer the exposure duration, the deeper the resetting of the luminescence signal into the rock surface (Habermann et al., 2000; Polikreti et al., 2002, 2003; Laskaris and Liritzis, 2011; Sohbati et al., 2011, 2012a; 2012b). Thus, there exists chronological information in the luminescence-depth profile, but the estimation of exposure time requires an independent knowledge of the  $\sigma\phi_0$  parameter, which is challenging to quantify from the first principles (Sohbati et al., 2011). One practical solution is to quantify the  $\sigma\phi_0$  and  $\mu$  parameters using a calibration sample of known age with similar lithological characteristics and exposure conditions as the dating sample (Sohbati et al., 2012a). Using this approach, Sohbati et al. (2012a) estimated the exposure time of multiple sandstone bedrock samples, thus constraining the age of an archaeologically-significant Barrier Canyon Style rock art in the southwestern USA (Chapot et al., 2012; Pederson et al., 2014). Despite several applications of the OSL-surf technique since then (e.g., Lehmann et al., 2018; Meyer et al., in press, other manuscripts in LED2017 proceedings), the bleaching-depth model (Eq. (1)) is yet to be validated experimentally; this is critical for further development of the technique.

The emerging OSL-surf technique has the potential to answer many new questions in the fields of geo- and archaeological sciences. One such new application is constraining the timing of exploitation of Palaeolithic stone quarry sites. These sites are boulders or bedrock outcrops from which humans systematically extracted stone for making artefacts. When a large flake is removed from the bedrock outcrop of a quarry, a fresh rock surface is exposed and the “OSL-exposure clock” begins to tick. The scars remaining on bedrock/boulder outcrops after flakes of sufficient thickness have been removed (flake scars) are, thus, potential targets for dating using an OSL-Surf technique.

In this study, we use the OSL-Surf dating technique to obtain a chronology for a stone tool quarry site in southern Tibet. We start by providing the first validation of the principles and model (Eq. (1)) using a controlled laboratory experiment. Subsequently, we estimate the exposure duration of an unknown-age surface and discuss possible controls on the  $\mu$  parameter value.

## 2. Sample description and measurement facilities

All experiments in this study were performed using rock samples collected from the lithic quarry site of Su-re in southern Tibet, which consists of a series of quartzite boulders exhibiting flake scars (Fig. 1a) and a surface scatter of flakes and cores. Multiple panels of quartzite exhibiting flake scars (Fig. 1a) were collected in 2014. Twenty months (1.667 a) later, the fresh rock surfaces that were created by sample collection in 2014 were sampled to obtain a suite of known-age rock surfaces (calibration scars: Fig. 1b). Additionally, boulder-sized samples were collected for laboratory bleaching experiments.

The quartzite is composed of quartz crystals that show shadowy extinction under cross-polarized light and very few feldspar grains (Fig. 1c – thin-section). The outer, light-exposed surfaces (depths > 4 cm) of the boulders were removed in safe light conditions (subdued red light) using a water-cooled rock saw. The remaining core of the boulder, which exists in luminescence field saturation, was then cut into cubes ( $\sim 3 \times 3 \times 3$  cm) for the laboratory bleaching experiment.

To measure OSL-depth profiles, cores (8.5 mm diameter) were drilled using a water-cooled diamond core drill. The cores (> 20 mm in length) were then sliced in 1 mm increments using a diamond wafering blade (0.3 mm thick) mounted on a Buehler low-speed saw, yielding slices that were  $\sim 0.7$  mm thick. The slices were then crushed with a mortar and pestle and the resulting grains were sieved to retain those with a diameter of 90–250  $\mu\text{m}$ . The grains were then mounted on stainless steel discs using a 5-mm mask ( $\sim 600$  grains per aliquot) and

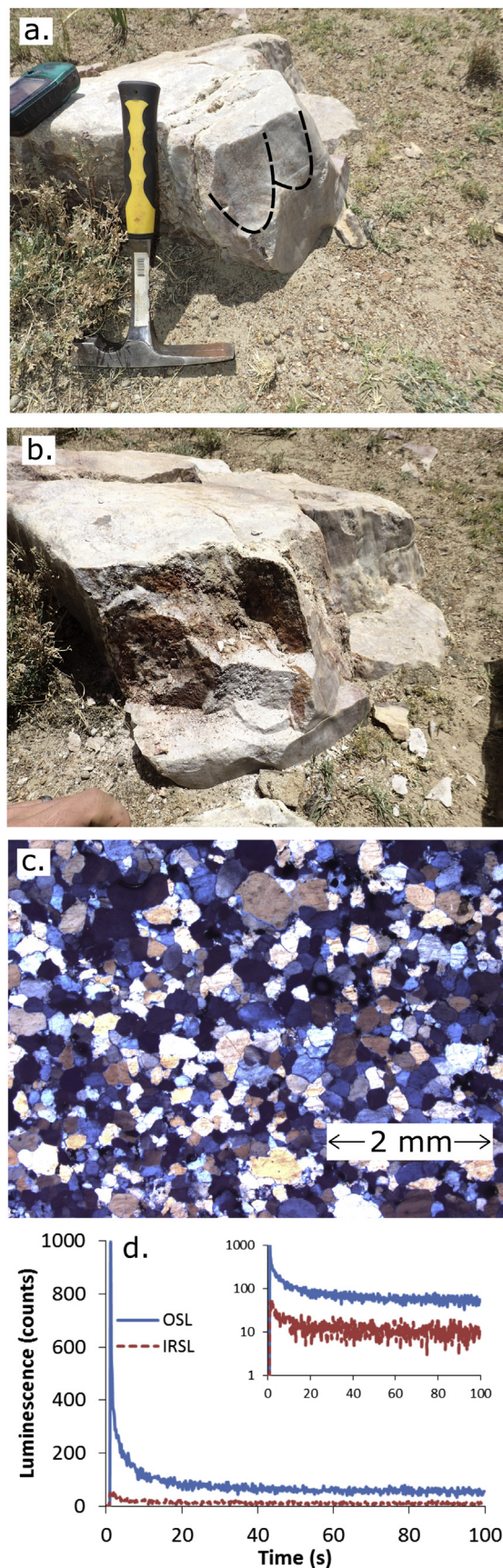


Fig. 1. Photo of sampled boulder with flake scar sample TIN-48 (a) and sampling scar collected 1.667 years later for model calibration (b). Cross polarized image of thin section of Su-re quartzite material (c). OSL and IRSL decay curves measured following a 40 Gy test dose irradiation from a multi-grain aliquot of crushed Su-re quartzite material (d). Inset shows same data on a log y-axis.

measured using a Risø TL/OSL DA20 reader (Bøtter-Jensen et al., 2010). Aliquots were stimulated using blue LEDs ( $470 \pm 30$  nm) following infrared (IR) (875 nm) stimulations in a post-IR OSL approach to ensure the purity of quartz OSL signal. Photons were measured using an Electron Tubes Ltd 9635 photomultiplier tube and the ultraviolet OSL emissions were measured through 7.5 mm of Hoya U-340 filter. IR stimulations were performed for 100 s at  $50^\circ\text{C}$ , and blue stimulations were performed for 100 s at  $125^\circ\text{C}$ . Signals were integrated using an early-background subtraction approach (signal summed between 0 and 1.0 s minus a background integrated between 1.0 and 3.6 s) (Cunningham and Wallinga, 2010). Laboratory irradiations were given using a calibrated  $^{90}\text{Sr}/^{90}\text{Y}$  beta source mounted on the Risø TL/OSL reader.

### 3. Luminescence characteristics and OSL-depth profiles

To investigate the luminescence properties of the Su-re quartzite, a dose recovery experiment was performed. Twenty-four aliquots were bleached in the solar simulator for two hours before being given surrogate natural doses ranging between 20 and 120 Gy. A single-aliquot regenerative dose (SAR; Murray and Wintle, 2000) procedure with a preheat of  $220^\circ\text{C}$  (10 s) for natural/regenerative-dose and test-dose, and post-IR OSL measurement was used to estimate equivalent dose values. The post-IR OSL signal from the measured aliquots is an order of magnitude brighter than the rather dim IRSL signals (Fig. 1d), corroborating thin-section observations of low feldspar content, and confirming that the measured OSL signal is dominated by emissions from quartz grains. The test dose OSL signal showed fast ratios (Durcan and Duller, 2011) ranging between 4 and 13, indicating the presence, but not dominance of the fast component. However, the dose recoveries yielded consistent measured/given dose ratios ( $1.01 \pm 0.02$ ,  $n = 24$ ) and recycling ratios ( $1.02 \pm 0.02$ ,  $n = 24$ ), and negligible recuperation ( $0.007 \pm 0.002$ ,  $n = 24$ ), suggesting that the post-IR OSL signal from Su-re quartzite has generally suitable luminescence characteristics and that the early background subtraction approach preferentially isolates a signal that is dominated by the fast component of quartz (Jain et al., 2003, 2005). These results indicate that the measurement conditions (e.g., preheats, test dose, etc.) are appropriate for accurate sensitivity correction and dose determination.

For OSL-depth profiles, the natural OSL signal from between three and six aliquots from each slice was measured. For each aliquot, the natural OSL signal ( $L_n$ ) was corrected by a test dose signal ( $T_n$ ) response to a 40 Gy test dose. For comparisons across different cores, the  $L_n/T_n$  ratio for each slice was normalised using the saturated  $L_n/T_n$  value from the same core (the weighted mean of the deepest five slices). For each exposed surface, two cores were used to measure OSL-depth profiles, and the weighted mean  $L_n/T_n$  from aliquots from each slice (e.g., slice 1 from Core 1 and Core 2) were used to create a single, averaged OSL-depth profile per exposed surface. Eq. (1) was fitted to the OSL-depth profiles in OriginPro using a least squares fitting approach employing the Levenberg-Marquardt algorithm.

### 4. Solar simulator bleaching experiment

Cubes ( $\sim 3 \times 3 \times 3$  cm) of Su-re quartzite material with saturated latent OSL signals were wrapped in aluminium foil, leaving one rock surface exposed, thus preventing light penetration via the sides of the cubes. All cubes were placed in the solar simulator (Hönle Sol 500) at the same time with their exposed surfaces placed perpendicular to, and at the same distance (120 cm) from, the light source. The cubes were then removed, one by one, after 1035 s, 10 ks, 50 ks, 100 ks, and 1040 ks. One additional cube was not placed in the solar simulator (0 s) and served as a control.

OSL-depth profiles for the two cores from each block are shown in Fig. 2. Firstly, the 0 s bleached curve is in saturation at all depths confirming that sufficient outer light-exposed material from the boulder

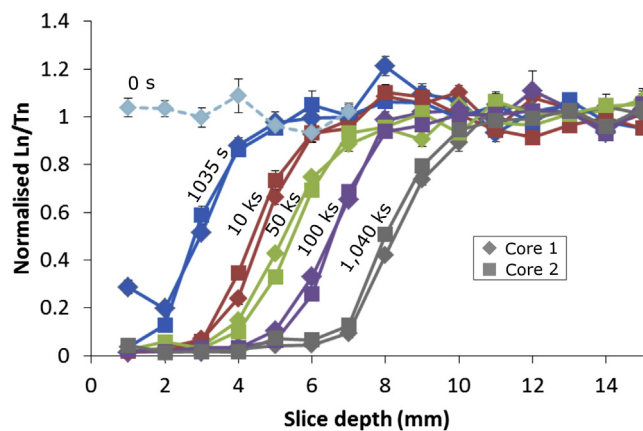
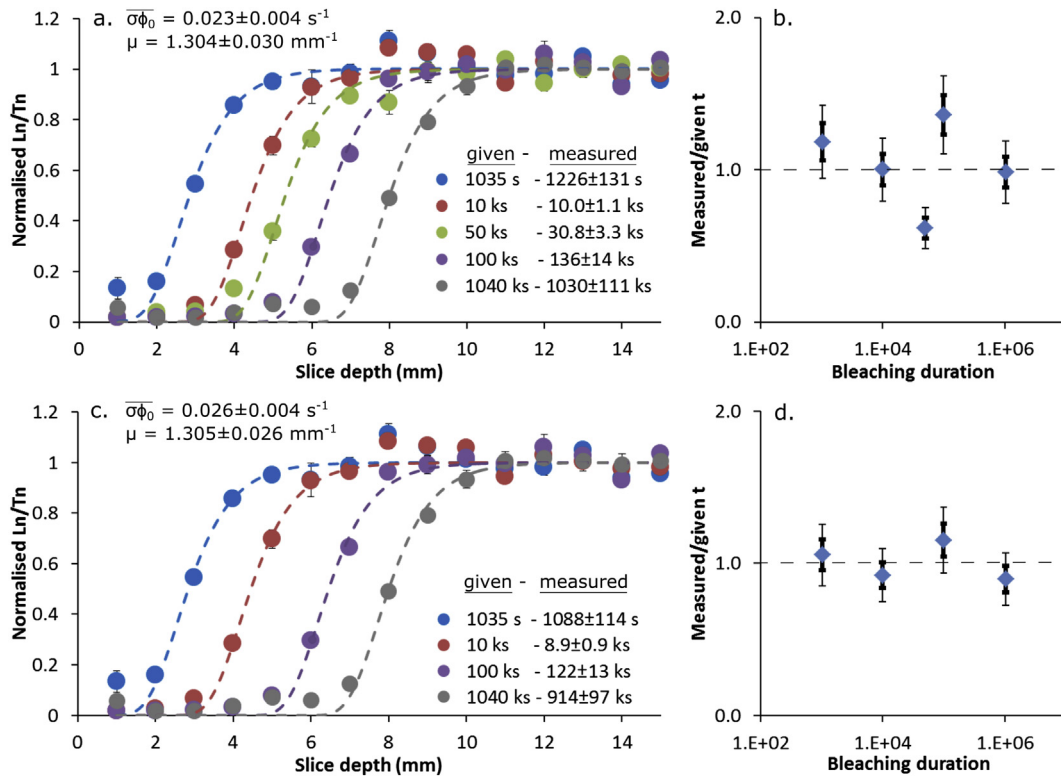


Fig. 2. OSL-depth profiles for each measured core from the laboratory bleaching experiment. Each data point is the weighted mean of between three and six aliquots.

was removed during cutting, and the subsequent slicing/coring procedure did not affect the OSL signal. Secondly, the replicate OSL-depth profiles are reproducible, and the depth of the bleaching front increases with bleaching duration in apparent qualitative agreement with the prediction of the OSL-surf model (Eq. (1)). In order to validate the model quantitatively, the replicate profiles from each cube were averaged as described in Section 3 and fitted to Eq. (1) using a two-step approach (Fig. 3a). First, since all cubes have the same lithology and bleaching conditions, the model parameters  $\mu$  and  $\overline{\sigma\varphi_0}$  should be shared for different profiles. A global fit of Eq. (1) (without using any weighting factor/scheme) to the average OSL-depth profile data fixing their known exposure times ( $t$ ) yielded  $\mu = 1.30 \pm 0.03 \text{ mm}^{-1}$  and  $\overline{\sigma\varphi_0} = 0.023 \pm 0.004 \text{ s}^{-1}$ . Second, Eq. (1) was again fitted to each cube's unweighted OSL-depth data, but this time the sample-specific  $\mu$  and  $\overline{\sigma\varphi_0}$  values determined in step 1 were fixed, and a modelled estimate for  $t$  (s) was determined by fitting (Fig. 3a legend). The ratio of the modelled to known  $t$  is plotted in Fig. 3b. A value consistent with unity would validate that the model data is accurately estimating the exposure duration. Three out of the five datasets (1035 s, 10 ks, and 1040 ks) yield modelled/known  $t$  ratios that are consistent with unity at  $2\sigma$ . However, the 50 ks and 100 ks samples yield inconsistent  $t$  estimates.

To further investigate these inaccurate  $t$  estimates and to assess the sensitivity of the model to the input data, the fitting was repeated twice with different constraints. First, Eq. (1) was fitted to each profile individually with the known  $t$  value constrained and profile-specific  $\mu$  and  $\overline{\sigma\varphi_0}$  values were determined (Table 1). It is clear from the data that the 50 ks  $\mu$  value is significantly different from the rest. Consequently, a second fit was performed in which the 50 ks data was excluded and the shared  $\mu$  and  $\overline{\sigma\varphi_0}$  estimates for the remaining profiles were determined. This time, all four datasets (1035 s, 10 ks, 100 ks, and 1040 ks) yielded modelled/known  $t$  ratios that are consistent with unity at  $2\sigma$  (Fig. 3c and d). These results indicate two important conclusions. First, the 50 ks OSL-depth profile cannot be accurately described using the  $\mu$  and  $\overline{\sigma\varphi_0}$  values that are appropriate for the other four samples. One possible explanation for this result is minor lithological differences in the opacity of the rock sample, perhaps due to the occasional presence of Fe coating planes inside the rock sample, which has been shown to vary within a given core and can significantly affect the shape of the OSL-depth profiles (Meyer et al., in press). Second, the net change in  $\mu$  and  $\overline{\sigma\varphi_0}$  parameter values is only  $0.0013 \text{ mm}^{-1}$  and  $0.003 \text{ s}^{-1}$ , respectively, when the 50 ks dataset is excluded (Table 1). While this small difference is within the uncertainties of the estimates, the new parameter values yielded accurate estimates of modelled  $t$  for the four fitted curves (Fig. 3d); this indicates that the model is highly sensitive to small variations in  $\mu$  and  $\overline{\sigma\varphi_0}$  parameters.



**Fig. 3.** Combined OSL-depth profile data and models for each block in the bleaching experiment (a) and for each block except the 50 ks bleached sample (c). Each data point is the weighted mean of between six and twelve aliquots. (b) and (d) show the measured/given  $t$  ratios derived from the fits shown in (a) and (c), respectively. Error bars are shown at  $1\sigma$  (bold) and  $2\sigma$ .

**Table 1**

Model parameters and results from fitting Equation (1) to the bleaching experiment OSL-depth profile data individually. The known  $t$ -value was constrained.

Given $t$	$\overline{\sigma\phi_0}$ ( $\text{s}^{-1}$ )	$\mu$ ( $\text{mm}^{-1}$ )
1035 s	$0.0166 \pm 0.0085$	$1.13 \pm 0.18$
10 ks	$0.0218 \pm 0.0175$	$1.29 \pm 0.18$
50 ks	$0.0016 \pm 0.0007$	$0.89 \pm 0.08$
100 ks	$0.0201 \pm 0.0218$	$1.24 \pm 0.17$
1040 ks	$0.0055 \pm 0.0053$	$1.13 \pm 0.12$

Additionally, we found that fitting Eq. (1) to our unweighted OSL-depth data yielded the best fits ( $r^2$  and residual sum of squares) and most accurate estimates of  $t$ . In this case, this is possibly because the most important part of the curve that governs the  $\mu$  and  $\overline{\sigma\phi_0}$  parameters is the bleaching front (i.e., the slices between fully bleached and saturated) and most weighting schemes favour very low values (e.g., statistical weighting:  $w = 1/y$ ) or high values (e.g., direct weighting:  $w = y(\text{err})$  or instrumental:  $w = 1/y(\text{err})^2$ ), thus yielding sub-optimal fitting results.

### 5. Naturally daylight-bleached flake scar dating

To date an unknown age rock surface, a known-age surface is needed to calibrate the  $\mu$  and  $\overline{\sigma\phi_0}$  parameters. Sample TIN2016-099 was the scar created by collecting sample TIN-48; it was collected 20 months (1.667 a) after exposure and served as the calibration sample for sample TIN-48 (Fig. 1a). A second known-age calibration sample (TIN2016-152) of identical lithology and exposure duration to TIN2016-099 was also measured, but was not used to calibrate the parameters for dating sample TIN-48 (see below). Unfortunately, sample TIN-48 was not thick enough; the  $L_n/T_n$  values still show an

increasing trend with depth without reaching a saturation plateau (though close within the 35 mm thickness of the sample). Consequently, the  $L_n/T_n$  saturation value from TIN-099 was assumed to reflect that of TIN-48, and was used to normalise the OSL-depth profiles. This assumption is sound given that both samples (i) come from the exact same boulder and the measured grains come from within 4 cm of each other laterally, and (ii) were measured on the same Risø TL/OSL reader using the same experimental conditions.

The combined OSL-depth profiles for TIN2016-099 and TIN-48 are shown in Fig. 4. To determine best-fit  $\mu$  and  $\overline{\sigma\phi_0}$  parameters, Eq. (1) was fitted to both samples' unweighted OSL-depth profiles simultaneously,

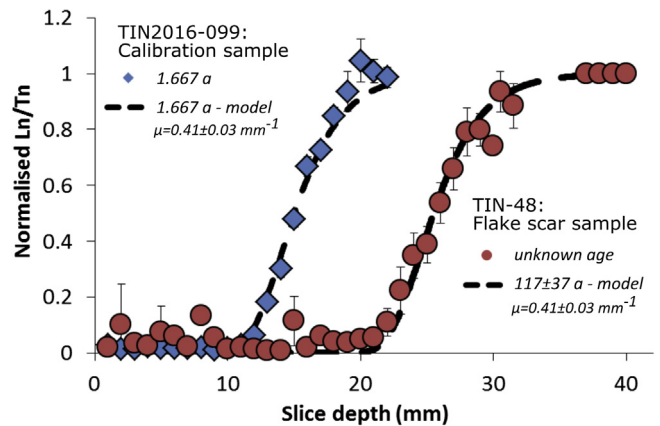


**Fig. 4.** Combined OSL-depth profiles and models for an unknown age sample (TIN-48; red) and a known-age (1.66 a) calibration sample (TIN2016-099; blue). Each point is the weighted mean of between two (slices 1–4 and slices 1–14 for TIN2016-099 and TIN-48, respectively) and six aliquots. (For interpretation of the references to colour in this figure legend, the reader is referred to the web version of this article.)

sharing the  $\mu$  and  $\overline{\sigma\varphi_0}$  parameters, constraining the known  $t$  value of TIN2016-099 to 1.667 a (i.e., 20 months), and leaving the unknown  $t$  value of TIN-48 unconstrained. The resulting best-fit parameter values (i.e.  $\mu = 0.41 \pm 0.03 \text{ mm}^{-1}$  and  $\overline{\sigma\varphi_0} = 186.2 \pm 80.3 \text{ a}^{-1}$ ) yielded an exposure duration of  $117 \pm 37$  a for sample TIN-48, providing the first direct age for human exploitation of the Su-re lithic quarry.

It should be noted that the Su-re quartzite is very transparent; the OSL signal is bleached to within 5% of saturation at depths of  $\sim 21$  mm and  $\sim 32$  mm after 1.667 a and 117 a, respectively. Furthermore, the best-fit  $\mu$  and  $\overline{\sigma\varphi_0}$  parameter values indicate that after 1 ka, 10 ka, and 100 ka the OSL signal will be bleached to within 5% of saturation at depths of 38 mm, 43 mm, and 49 mm, respectively. For the OSL-Surf technique to be successfully applied to date quarries, it is crucial that the flakes detached from boulders be thick enough to remove all material with a bleached OSL signal. When quarries are exploited, large pieces of rock are generally detached from quarried boulders to serve as cores from which flakes are removed to manufacture tools. Therefore, the dimensions of the flakes scattered around the quarry site are unlikely to approximate the true thickness of material removed from the boulders. However, the thickness of cores remaining at the site may serve as a minimum estimate of the material detached from the boulders. A subsample of the scattered lithic material at the site yields thicknesses ranging from 1 to 7 cm. The largest two lithics (6 and 7 cm thickness) are cores that are thick enough to have removed the bleached surfaces of the quarried boulder, thus revealing flake scars in luminescence field saturation.

## 6. Factors controlling light attenuation

It is interesting to note that the best-fit  $\mu$  value for the naturally daylight-bleached samples is very different to that of the laboratory-bleached samples. This difference in  $\mu$  reflects the different shapes of the OSL-depth profiles (see the comparison in Fig. 5a). Considering that (i) the  $\mu$  parameter is lithology-specific and (ii) both datasets were measured using rocks of the same lithology, one expects that the best-fit  $\mu$  values would be the same for both datasets. These results suggest that, in addition to lithological controls, the  $\mu$  parameter must be sensitive to the geometry and/or wavelength spectrum of the incident light. The laboratory bleaching experiments give insight into the potential dependence of  $\mu$  derived from the profile on wavelength. This observed  $\mu$  is a function of both the relative intensities as well as the true  $\mu$  values of the individual wavelength components in the rock. Assuming that the wavelength spectrum changes due to attenuation with depth into a rock, if the wavelength effect is significant then one would expect to observe different  $\mu$  values for samples of identical lithology with different exposure times. In other words, the observed  $\mu$  should vary with the depth to which the luminescence is reset. However, the observed  $\mu$  values in our various laboratory bleaching profiles are very similar (Table 1), in apparent contradiction with our assumption. But this observation is not surprising considering that quartz is a very pure mineral phase and transparent to wavelengths from deep UV to IR (bandgap  $\sim 9$  eV; Quinn et al., 2003). Thus, any attenuation in quartzite must mainly arise from scattering, reflection and minor absorption due to low-concentration defects, suggesting a weak dependence of  $\mu$  on wavelength. Furthermore, the ionisation cross-section(s) of the trap(s) responsible for OSL decrease exponentially with the energy of the incident photons (Bøtter-Jensen et al., 1994; Singarayer and Bailey, 2004; Meyer et al., in press). A combination of these two effects suggests that bleaching within quartzite must effectively be due to a relatively narrow wavelength band (UV-green) where dependence of  $\mu$  on wavelength is not likely to be very strong. Alternatively, the difference in  $\mu$  between our laboratory-bleached and naturally daylight-bleached profiles may be related to the difference in irradiation geometry, perpendicular vs.  $2\pi$ , respectively. A comparison of two calibration samples can address this. TIN2016-152 and TIN2016-099 have identical lithologies and exposure durations, and similar opacity variation with depth

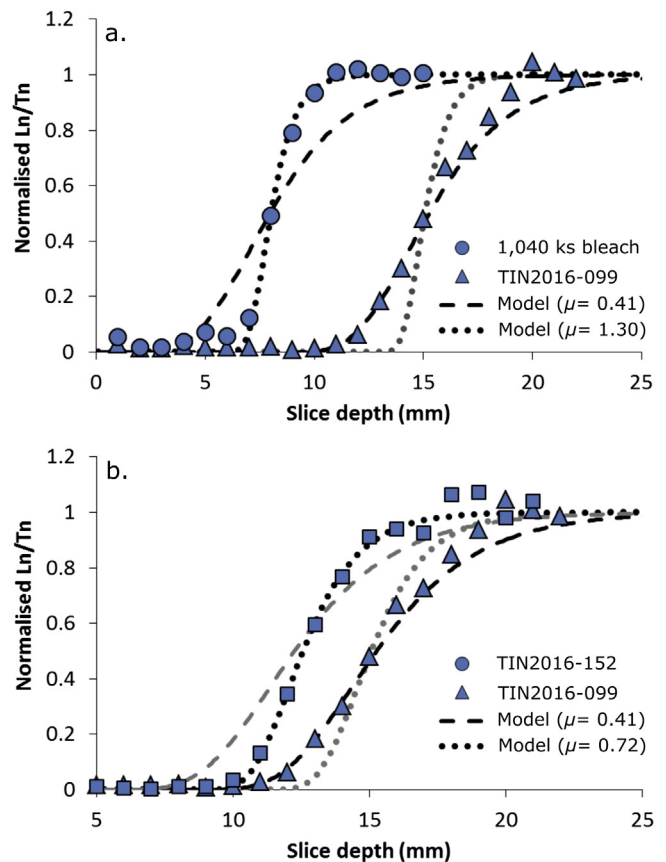


Fig. 5. (a) OSL-depth profiles for naturally daylight-bleached samples TIN2016-099 and the 1040 ks laboratory-bleached sample with Equation (1) fitted to the data, fixing  $\mu$  at  $0.40$  and  $1.30 \text{ mm}^{-1}$ . (b) OSL-depth profiles for naturally daylight-bleached samples TIN2016-099 and TIN2016-152 with Equation (1) fitted to the data, fixing  $\mu$  at  $0.41$  and  $0.72 \text{ mm}^{-1}$ .

(Meyer et al., in press), but different orientations; TIN2016-099 is vertically oriented with a NW aspect and TIN2016-152 is sub-horizontally oriented with a SW aspect. While TIN2016-099 yielded a best fit  $\mu$  value of  $0.41 \pm 0.03 \text{ mm}^{-1}$ , TIN2016-152 yields a best-fit  $\mu$  value of  $0.72 \pm 0.06 \text{ mm}^{-1}$  (Fig. 5b). These results show that the specific irradiation geometry due to exposure aspect has a measurable effect on the  $\mu$  value and thereby the shape of the OSL-depth profile. From a practical point of view, these results suggest (i) that  $\mu$  parameter values determined in the laboratory may not necessarily reflect those of natural samples if the irradiation geometry is not taken into consideration, and (ii) that  $\mu$  parameter values can vary for samples of identical lithology, depending on daylight irradiation geometry; thus the choice of calibration sample must be considered very carefully.

## 7. Conclusions

In this study we investigated the feasibility of using the newly developed OSL-Surf dating approach to date flake scars at lithic quarry sites. We performed the first validation of the principles and mathematics that underlie the OSL-Surf dating technique using a controlled laboratory experiment. Our results show that longer exposure durations yield deeper reset OSL-depth profiles in homogenous material. Thus, the OSL-Surf approach can be used as a relative dating tool to differentiate different age rock surfaces, where the lithology and local daylight irradiation conditions (i.e., aspect, shadowing, etc.) are comparable. Our efforts towards quantitative validation of the model show that model predictions are highly sensitive to the parameter values. One sample (50 ks) was shown to be best fitted by a  $\mu$  value that significantly

differed from the rest of the samples – possibly because of small-scale differences in opacity between the samples due to, perhaps, the presence of Fe coating planes. When this 50 ks sample was treated as an outlier, the OSL-surf model fitted to the OSL-depth profile data from the remaining four samples yielded accurate estimates of known-exposure-duration within  $2\sigma$ .

In addition to validating the OSL-Surf dating model, we could determine the exposure age of an unknown-age rock surface that is related to human exploitation of a lithic quarry site. The problem of finding a suitable calibration sample was solved by revisiting the site and collecting the scar remaining after earlier sample collection. This calibration sample has a precisely known exposure age of 1.667 a and yielded a measurable OSL-depth profile that could be used to estimate the exposure duration of 117 a for the flake scar associated with human exploitation of the area.

Surprisingly, the laboratory-bleached dataset and the two naturally daylight-bleached datasets yielded very different best-fit light attenuation coefficients ( $\mu$  parameter values). This suggests that, in addition to lithological controls and possibly the irradiating light's wavelength spectrum, the  $\mu$  parameter is sensitive to the orientation of the incident light, with the laboratory-bleaching and natural daylight-irradiation in perpendicular and  $2\pi$  geometries, respectively. Indeed, even two different exposure geometries in nature were shown to yield significantly different best-fit  $\mu$  values for samples of identical lithology and exposure duration from the same site. From the practical point of view, these results suggest that  $\mu$  parameter values determined in the laboratory do not necessarily reflect those of natural samples and that known-age calibration samples should replicate unknown-age samples as closely as possible in lithology and specific exposure geometries. Conversely, the comparison of  $\mu$  values between the calibration and dating samples may be used as one of the tests to verify the field calibration procedure.

## Acknowledgements

This research was funded by an Austrian Science Fund grant to L.A.G. (FWF-M2121-G25) and M.C.M. (FWF grant 24924-G19). Jan-Hendrik May and Mark Aldenderfer are thanked for their assistance in the field, Kornelia Pellegrini is thanked for her assistance in the laboratory, and an anonymous reviewer is thanked for their comments which improved the quality of this manuscript.

## References

Bøtter-Jensen, L., Duller, G.A.T., Poolton, N.R.J., 1994. Excitation and emission

- spectrometry of stimulated luminescence from quartz and feldspars. *Radiat. Meas.* 23 (2–3), 613–616.
- Bøtter-Jensen, L., Thomsen, K.J., Jain, M., 2010. Review of optically stimulated luminescence (OSL) instrumental developments for retrospective dosimetry. *Radiat. Meas.* 45, 253–257.
- Chapot, M.S., Sohbati, R., Murray, A.S., Pederson, J.L., Rittenour, T.M., 2012. Quaternary Geochronology Constraining the age of rock art by dating a rockfall event using sediment and rock-surface luminescence dating techniques. *Quat. Geochronol.* 13, 18–25.
- Cunningham, A.C., Wallinga, J., 2010. Selection of integration time intervals for quartz OSL decay curves. *Quat. Geochronol.* 5, 657–666.
- Durcan, J.A., Duller, G.A.T., 2011. The fast ratio: a rapid measure for testing the dominance of the fast component in the initial OSL signal from quartz. *Radiat. Meas.* 46, 1065–1072.
- Habermann, J., Schilles, T., Kalchgruber, R., Wagner, G.A., 2000. Steps towards surface dating using luminescence. *Radiat. Meas.* 32, 847–851.
- Jain, M., Murray, A.S., Bøtter-Jensen, L., 2003. Characterisation of blue-light stimulated luminescence components in different quartz samples: implications for dose measurement. *Radiat. Meas.* 37, 441–449.
- Jain, M., Murray, A.S., Bøtter-Jensen, L., Wintle, A.G., 2005. A single-aliquot regenerative-dose method based on IR (1.49 eV) bleaching of the fast OSL component in quartz. *Radiat. Meas.* 39, 309–318.
- Laskaris, N., Liritzis, I., 2011. A new mathematical approximation of sunlight attenuation in rocks for surface luminescence dating. *J. Lumin.* 131, 1874–1884.
- Lehmann, B., Valla, P.G., King, G.E., Herman, F., 2018. Investigation of OSL surface-exposure dating to reconstruct post-LIA glacier fluctuation in the French Alps (Mer de Glace, Mont-Blanc massif). *Quat. Geochronol.* 44, 63–74.
- Meyer, M.C., Gliganic, L.A., Jain, M., Sohbati, R., 2018. Lithological controls on light penetration into rock surfaces – implications for OSL and IRSL surface exposure dating. *Radiat. Meas. (LED proceedings)*, (in press). <https://http://dx.doi.org/10.1016/j.radmeas.2018.03.004>.
- Murray, A.S., Wintle, A.G., 2000. Luminescence dating of quartz using an improved single-aliquot regenerative-dose protocol. *Radiat. Meas.* 32, 57–73.
- Pederson, J.L., Chapot, M.S., Simms, S.R., Sohbati, R., Rittenour, T.M., Murray, A.S., Cox, G., 2014. Age of Barrier Canyon-style rock art constrained by cross-cutting relations and luminescence dating techniques. *Proc. Natl. Acad. Sci. Unit. States Am.* 111, 12986–12991.
- Polikreti, K., Michael, C.T., Maniatis, Y., 2003. Thermoluminescence characteristics of marble and dating of freshly excavated marble objects. *Radiat. Meas.* 37, 87–94.
- Polikreti, K., Michael, C.T., Maniatis, Y., 2002. Authenticating marble sculpture with thermoluminescence. *Ancient TL* 20, 11–18.
- Quinn, F., Poolton, N.R.J., Malins, A., Pantos, E., Andersen, C., Denby, P., Dhanak, V., Miller, G., 2003. The mobile Luminescence End-Station, MOLES: a new public facility at Daresbury synchrotron. *J. Synchrotron Radiat.* 10 (6), 461–466.
- Singarayer, J.S., Bailey, R.M., 2004. Component-resolved bleaching spectra of quartz optically stimulated luminescence: preliminary results and implications for dating. *Radiat. Meas.* 38 (1), 111–118.
- Sohbati, R., Jain, M., Murray, A.S., 2012b. Surface exposure dating of non-terrestrial bodies using optically stimulated luminescence: a new method. *Icarus* 221, 160–166.
- Sohbati, R., Murray, A.S., Chapot, M.S., Jain, M., Pederson, J., 2012a. Optically stimulated luminescence (OSL) as a chronometer for surface exposure dating. *J. Geophys. Res.* 117, B09202.
- Sohbati, R., Murray, A.S., Jain, M., Buylaert, J.-P., Thomsen, K.J., 2011. Investigating the resetting of OSL signals in rock surfaces. *Geochronometria* 38, 249–258.